

# On the Inherent Memory Behavior in Electric Double Layer Capacitors under Different Levels of Noise

Anis Allagui\*

*Dept. of Sustainable and Renewable Energy Engineering,  
University of Sharjah, Sharjah, United Arab Emirates<sup>†</sup>*

Di Zhang

*Dept. of Sustainable and Renewable Energy Engineering,  
University of Sharjah, PO Box 27272, Sharjah, United Arab Emirates<sup>‡</sup>*

Ahmed S. Elwakil

*Dept. of Electrical and Computer Engineering, University of Sharjah,  
PO Box 27272, Sharjah, United Arab Emirates<sup>§</sup>*

(Dated: July 1, 2022)

The capacitive memory effects in the dynamic response of electric double-layer capacitors (EDLCs) that integrate its cumulative history of stimulation and state have been observed and reported in several recent studies. The excitation signals used to detect such behavior are usually of different nature (e.g. constant voltage vs. linear voltage) and different durations with the objective of charging the device to the same voltage-charge point, and from which the discharge patterns are studied. The aim of this work is to provide a new experimental evidence of the inherent memory effect in EDLCs in response to time-varying stationary input excitations with different statistical properties. Specifically, we engineered different sets of charging voltage waveforms composed of fixed dc values on top of which we superimposed uniformly-distributed fluctuations of different amplitudes (different noise levels). The duration of the signals remains the same for different values of variance around the mean value. We observed different time-charge responses depending on the extent of the noise level in the voltage-charging waveforms. This can be explained in the context of inherent memory effects using fractional-order constitutive relations of non-ideal capacitors that apply to EDLCs. We found that high variance noise signals make the device operate in less capacitive, more resistive mode, and thus with a stronger weighted sum of its voltage input prior history.

## I. INTRODUCTION

Supercapacitor are electrochemical energy storage devices known for their outstanding power performance, excellent reversibility and long cycle life, but they are still lagging behind in terms of energy density when compared with batteries. Their charge storage mechanisms can be either physical, i.e. purely electrostatic ion adsorption in the electric double-layer at the electrode/electrolyte interface, or pseudocapacitive via highly reversible and relatively fast redox reactions, or both. Furthermore, the transport dynamics in such devices in response to an external excitation is mainly subdiffusive [1], which can be attributed to several factors. This includes the porous nature of the electrodes and their fractal geometries, and thus some sort of spatial restriction subjected onto the

mobile ions, and also because of internal friction forces and continuous scattering of these ions while diffusing in the supporting electrolytes and through the wetted pores [2]. In addition, the different types of inter-ion interactions, crowdedness and buffering in narrow pores also play relevant roles in the establishment of retarded diffusion processes in such type of devices [1]. From a system-level perspective, the dynamics of the device follow a power-law behavior which can be viewed as the collective result of coupled processes with different, widely separated time constants, each of which follows for instance an exponential process [3–5]. Such multiple time scale dynamics may hint at the existence of some sort of memory effects that take into account the global, non-local time behavior of past activities up to the current time. This type of behavior, whether regarded from the time domain or the frequency domain points of view, can be well described with fractional-order integro-differential equations [6–13].

Some recent experimental investigations have demonstrated the history-dependent behavior of supercapacitors. The authors of this work showed in ref. [9] that discharging a supercapacitor (electric double-layer capacitor, EDLC) into a constant resistor from the same voltage-charge point reached using two different charging waveforms (step voltage and linear voltage ramp) of two different durations leads to two different responses,

---

\* aallagui@sharjah.ac.ae

<sup>†</sup> Center for Advanced Materials Research, Research Institute of Sciences and Engineering, University of Sharjah, PO Box 27272, Sharjah, United Arab Emirates

<sup>‡</sup> Center for Advanced Materials Research, Research Institute of Sciences and Engineering, University of Sharjah, PO Box 27272, Sharjah, United Arab Emirates; zdi@sharjah.ac.ae

<sup>§</sup> Nanoelectronics Integrated Systems Center (NISC), Nile University, Cairo, Egypt; Dept. of Electrical and Computer Engineering, University of Calgary, Calgary, Canada; elwakil@ieee.org

mostly in the short term, transient regime. This indicates that contrary to ideal capacitors, knowledge of the initial condition on an EDLC in terms of voltage and charge is not sufficient to determine its current and subsequent states. Knowledge of the charging pre-history also matters when modeling such devices. In a second study [10], we provided a quantitative estimate of the memory effect using the voltage memory trace interpretation of fractional-order dynamics [14]. A follow-up paper by the same group illustrated the application of the memory effect in supercapacitors by sequentially encoding information into the charging pattern of the device, and then uniquely retrieving this code from the discharge response [11].

Clearly supercapacitors (at least of the ELDC type) are dynamic entities with non-static mapping of input to output, contrary to the case of ideal capacitors. In this work we further investigate the memory effect and dynamic encoding of stimulus history of supercapacitors, albeit in response to time-varying stationary voltage excitations. The input voltage waveforms are derived from uniform distributions of different sample ranges, means and variances. It has been observed that the device carries additional information beyond just the mean value of the applied voltage input. The extent of the noisy excitation around the mean value and thus the prehistory and features of the charging sequence determine the actual response of the device at a given time. The cross correlation function between charge and voltage show a visible degree of correlation, and thus short term memory effects, that fade out as the time lag is increased. We also discuss the effect of noise variance on the weighted sum memory trace that takes into account all prior history of the device.

## II. METHODS

The electrical measurements were conducted on a commercial 1 F, 2.7 V GHC NanoForce supercapacitor using a Biologic VSP-300 electrochemical station equipped with an impedance spectroscopy module [15]. The source-measure instrument has a voltage resolution of  $1\mu\text{V}$  on 60 mV, voltage accuracy  $< \pm 1$  mV, and maximum voltage scan rate of 0.2 V/ms. The current range of the instrument is 10 nA to 1 A with lowest current accuracy and resolution of  $\pm 100$  pA and 0.8 pA, respectively, on 10 nA range.

For assessing the device's memory effect, excitation voltage signals of the type:  $v(t) = v_0 H(t) + (v_1 - v_0) H(t - t_1) + \dots + (v_n - v_{n-1}) H(t - t_n)$  (Eq. 7 below) were programmed to have 64 different settings by full factorial of four different voltage input mean values ( $V_{dc} = \mu = 0.5, 1.0, 1.5$  and  $2.0$  V) with four different ranges of uniformly-distributed voltage fluctuations (i.e. ranges of  $\pm 20, \pm 50, \pm 200$  and  $\pm 500$  mV) superposed on top of the dc values, and four different durations ( $\Delta t = 1, 5, 20$  and 60 seconds). Uniform noise means the signal contains

random values derived from a uniform distribution of probability density function expressed in terms of mean  $\mu_v = \mu$  and variance  $\sigma_v^2 = \sigma^2$  as:

$$f_1(x) = \begin{cases} \frac{1}{2\sqrt{3}\sigma}, & -\sqrt{3}\sigma \leq x - \mu \leq \sqrt{3}\sigma \\ 0, & \text{elsewhere} \end{cases}$$

that is, every value in the range or sample space is equally likely to occur. The values are also uncorrelated and independent. If we denote by  $a$  and  $b$  the lower and upper boundaries of the uniformly-distributed voltage excitations, that is

$$f_2(x) = \begin{cases} \frac{1}{b-a}, & a \leq x \leq b \\ 0, & \text{elsewhere} \end{cases}$$

then the variance  $\sigma^2 = (b-a)^2/12$  takes the values of  $(0.13, 0.83, 13.3, \text{ and } 83.3) \times 10^{-3} \text{ V}^2$  for the ranges  $\pm 20, \pm 50, \pm 200$  and  $\pm 500$  mV, respectively. Each signal consisted of  $N = 1000$  points equispaced in time with a time step of  $\Delta = T/N$ . Prior to each applied excitation, the device was discharged down to 5 mV with a constant resistor of  $10 \Omega$ .

## III. RESULTS

Before we analyze the time-domain measurements and the memory effects associated with the supercapacitor dynamics in response to the noisy voltage excitations, we first characterize the passive response of the device by impedance spectroscopy. We recall that the impedance of a linear, time-invariant system is defined as the ratio of the Laplace transforms of voltage by current as:

$$Z(s) = \frac{\mathcal{L}(v(t))}{\mathcal{L}(i(t))} = \frac{V(s)}{I(s)} \quad (1)$$

where  $s = j\omega$ . We used traditional stepped sine excitations of frequencies from 10 mHz up to 100 kHz with a small amplitude of 10 mV around a given dc voltage bias. The measurements were carried out using the Biologic VSP-300 station. The results in terms of Nyquist representation of real vs. imaginary parts of impedance, and impedance phase angle vs. frequency at 0, 0.9, 1.8 and 2.7 Vdc are shown in Fig. 1. In both figures, there are clear deviations of the spectral impedance data of the device from that expected for ideal capacitors [16], i.e. non-vertical real vs. imaginary parts and phase angle above  $-90^\circ$ , which keeps increasing with the frequency.

The data in Fig. 1 can be fitted well enough with simple circuits that include the fractional, constant phase element (CPE) type of impedance (results are not shown here, see [16] for more details). The CPE impedance function is given by:

$$Z_{\text{CPE}} = \frac{1}{C_\alpha s^\alpha} \quad (2)$$

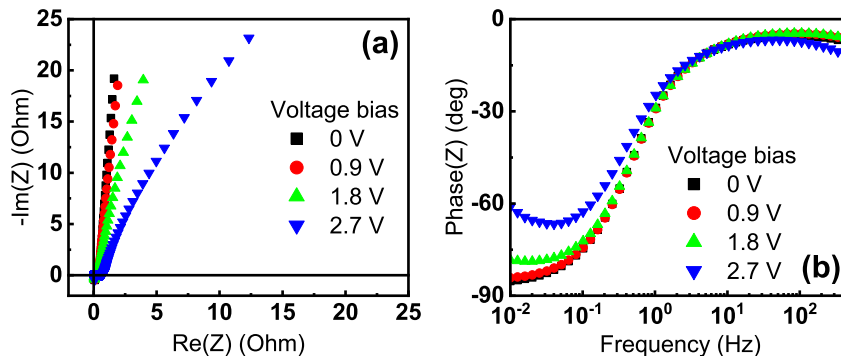


FIG. 1. Impedance spectroscopy results of the GHC NanoForce supercapacitor (rated 1 F, 2.7 V)

where  $s^\alpha = \omega^\alpha \angle \alpha\pi/2$ , and  $0 < \alpha \leq 1$ , which reduces to the impedance of an ideal capacitor  $1/(C_1 s)$  when  $\alpha = 1$ . This indicates *a priori* that memory effects should be expected in time-domain experiments. We note in this regard that by inverse Laplace transformation, the voltage-current relationship corresponding to Eq. 2 is [9, 10, 17, 18]:

$$i(t) = C_\alpha {}_0^C D_t^\alpha v(t) \quad (3)$$

instead of  $i(t) = C_1 dv(t)/dt$  as known for ideal capacitors. Here, the operator  ${}_0^C D_t^\alpha$  represents the right-sided Caputo time fractional derivative of order  $\alpha > 0$  defined by the integro-differential relation:

$${}_0^C D_t^\alpha f(t) = \frac{1}{\Gamma(m-\alpha)} \int_0^t (t-\tau)^{-\alpha-1+m} f^{(m)}(\tau) d\tau \quad (4)$$

where  $m-1 < \alpha \leq m$ ,  $m \in \mathbb{N}$ , and  $f^{(m)}(\tau)$  is the  $m^{\text{th}}$  derivative of  $f(\tau)$ . The integral indicates, as we shall discuss below in more detail, that all prior history of the function should be accounted for in order to determine the actual behavior of the function at a given time  $t$ .

Typical results depicting the memory effect observed with the supercapacitor device are shown in Fig. 2. We show in Fig. 2(a) the plots of 20-second-long voltage input excitations of 0.5 V in mean value with the four different superposed uniformly-distributed fluctuations within the ranges  $\pm 20$ ,  $\pm 50$ ,  $\pm 200$  and  $\pm 500$  mV (i.e. 40, 100, 400, 1000 mV<sub>pp</sub>). The last value of each charging sequence is appended to 0.5 V. The results obtained for other dc voltage values, other durations and with the same superimposed fluctuations are similar to those in Fig. 2, and therefore are not shown here. The corresponding accumulated charges in mA.h in response to the voltage excitations in Fig. 2(a) are given in Fig. 2(b). The overall trends of the curves start first with a relatively quick power law-like growth of the accumulated charge (not necessarily exponential [19]), followed by an asymptotic limit as the charging time is increased. We also observe from this quasi-stationary signal that in response to a sudden change of a voltage stimulus, the device responds accordingly with relatively large change in

the instantaneous charge followed by slower adaptation to steady state until the next change in voltage input (Fig. 2(c)). Of course, an increase of charge is observed when a step up voltage is applied, and vice versa, a decrease of charge is observed when a step down voltage is applied. The overall extent of change in the accumulated charge superposed on the general trend is accentuated by the increase in variance of the input voltage signal (Fig. 2(b) and Fig. 2(c)). This leads to the primary important conclusion that the device's accumulated charge adapts to changes in the stimulus statistics, not only in terms of its mean value (results for other dc voltage values are similar and therefore are not show here), but also in its variance. This can be explained on the basis of the device's remnant memory of past activity [20], and the fact that EDLCs, because of their internal structure and mechanisms, are dynamical entities operating on distributions of time scales.

The results in Fig. 2 show also that by the end of the charging period the overall accumulated charges are slightly different from each other even though the last value of voltage is set to 0.5 V. The same is observed for the other tested scenarios, i.e. with different mean values and different excitation durations.

Plots of the point-by-point ratios of charge to voltage, and plots of normalized cross-correlations between voltage and charge for the different levels of noise used are shown in Fig. 2(d) and 2(e), respectively. The cross-correlations is defined as:

$$R_{vq}(\tau) = E \{v(t) q(t + \tau)\} \quad (5)$$

where  $E\{\cdot\}$  denotes the expected value. The charge-voltage correlation as a function of time lag when the voltage input signal is superposed with  $\sigma^2 = 83.3 \times 10^{-3} \text{ V}^2$  always shows lower values compared to the cases with lower variance values, in addition to some nonlinearities observed with shorter time lags. This indicated a lack of correlation between the two variables and thus the invalidity of the constitutive relation  $\Delta q(t) = C_1 \Delta v$ , which should be applied for the case of ideal capacitors only [21–23].

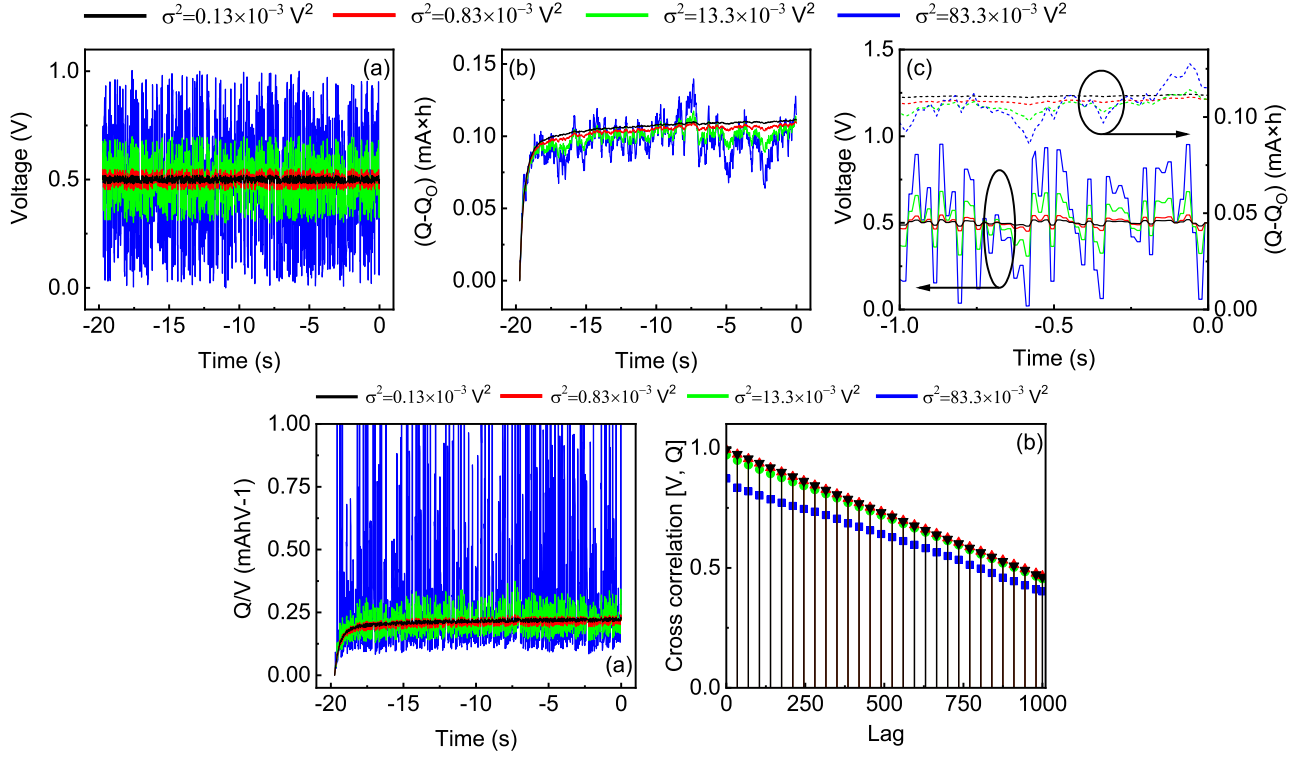


FIG. 2. Typical time-domain charge response (b) of the the GHC NanoForce supercapacitor (rated 1 F, 2.7 V) when excited with voltage waveforms (a) derived from uniform distributions of different sample ranges and variances (mean value of 0.5 Vdc in this case). In (c) we show the synchronized voltage and charge vs. time for the last second of the experiment. (d) Plot of the ratio  $\Delta q/\Delta v$  vs. time and (e) plot of  $R_{vq}(\tau)$  (Eq. 5) vs. number of time lags

Furthermore, the correlation coefficient defined as:

$$\rho_{vq} = \frac{\text{Cov}\{v, q\}}{\sigma_v \sigma_q} \quad (6)$$

where  $\text{Cov}\{\cdot\}$  denotes the covariance between  $v$  and  $q$  are found to be -0.0491, -0.0297, 0.0684 and 0.2141 for the four different signals with superposed uniformly-distributed fluctuations within the ranges  $\pm 20$ ,  $\pm 50$ ,  $\pm 200$  and  $\pm 500$  mV, respectively. The highest value of  $\rho_{vq}$  goes with the highest variance of noise.

#### IV. DISCUSSION

In order to relate the inherent memory behavior observed in the dynamic response of dissipative EDLCs we analyze the results above with concepts borrowed from fractional calculus. We consider a linear capacitive device subjected to a time-varying voltage excitation  $v(t)$  represented by a series of step inputs each of which begins at different time, such that:

$$\begin{aligned} v(t) = & v_0 H(t) \\ & + (v_1 - v_0) H(t - t_1) + \dots \\ & + (v_k - v_{k-1}) H(t - t_k) \end{aligned} \quad (7)$$

where  $H(t - t_k)$  is the Heaviside step function. The resulting electrical charge developed by the device in this case, assumed to satisfy the superposition principle, can be represented as a sum of the output for each individual step as follows:

$$\begin{aligned} q(t) = & c(t)v_0 H(t) \\ & + c(t - t_1)(v_1 - v_0) H(t - t_1) + \dots \\ & + c(t - t_n)(v_k - v_{k-1}) H(t - t_k) \end{aligned} \quad (8)$$

where  $c(t - t_k)$  is a capacitive operator that characterizes the device and maps inputs into outputs [21]. In such a time-domain model, each output is a delayed and scaled copy of the input signal. In series form we can rewrite the charge as:

$$\begin{aligned} q(t) = & c(t)v_0 H(t) \\ & + \sum_n c(t - t_k)(v_k - v_{k-1}) H(t - t_k) \end{aligned} \quad (9)$$

Multiplying and dividing by the time increment  $\Delta\tau$  between each step, and taking the limit as  $k$  approaches infinity and  $\Delta\tau$  approaches zero, one obtains the follow-

ing result for the charge:

$$q(t) = c(t)v_0H(t) + \lim_{\substack{k \rightarrow \infty \\ \Delta\tau \rightarrow 0}} \sum_k c(t-t_n) \frac{(v_k - v_{k-1})}{\Delta\tau} H(t-t_k) \Delta\tau \quad (10)$$

or in terms of a hereditary (convolution) integral as [20, 24]:

$$q(t) = c(t)v_0H(t) + \int_0^t c(t-\tau) \frac{dv}{d\tau} d\tau \quad (11)$$

The integral indicates again (Eq. 4) that all events over the history of the device contribute to its current state, or specifically, the resulting charge in the device at a time  $t$  depends on the change in applied voltage taken at times in the interval  $\tau \in [0, t]$  weighted by the convolution kernel  $c(t-\tau)$ . Note that the lower limit of the integral in Eq. 11 can be taken to be  $-\infty$  to reflect infinite past.

For the particular case of an ideal capacitor of capacitance that does not change upon variations in the applied voltage or frequency, we write the kernel function  $c(t-\tau)$  that relates voltage to charge as  $c(t-\tau) = C_1$  where  $C_1$  is a constant. Thus, Eq. 11 turns to be the well-known constitutive relation  $\Delta q(t) = C_1 \Delta v$  where  $\Delta q(t)$  is evidently equal to  $q(t) - c(t)v_0H(t)$ .

However, this is not the case with electrochemical capacitors or supercapacitors including EDLCs, pseudocapacitors and hybridized versions of the two. As mentioned above, due to their complex structures, inhomogeneities and porosities of their electrodes, and the presence of traps and obstacles leading to distributed waiting times, these devices have been shown to exhibit some sort of device hereditariness that takes into account the past activities up to the current time [6–8]. The charging or discharging processes depend not only on the initial conditions, as it is the case for ideal capacitors, but also on the entire prehistory. Again, this has been verified experimentally on a number of commercial supercapacitors using different excitation functions, and modeled with fractional-order integro-differential equations [9–11].

In fact, looking at the Caputo fractional derivative given by Eq. 4, we note that Eq. 11 has the same form as Eq. 4 when  $m = 1$  (i.e.  $0 < \alpha \leq 1$ ) and  $c(t)$  is the power law function

$$c(t) = \frac{C_\alpha}{\Gamma(1-\alpha)} t^{-\alpha} = \frac{C_0}{\Gamma(1-\alpha)} \left(\frac{t}{\tau_0}\right)^{-\alpha} \quad (12)$$

that tends to zero as  $t \rightarrow \infty$ . Here  $C_\alpha = C_0\tau_0^\alpha$  is the device pseudo-capacitance (not to be confused with pseudocapacitive materials or devices) and  $\tau_0$  is an arbitrary scaling time. Thus, a generalized charge-voltage relationship can be written as:

$$\Delta q(t) = C_0\tau_0^\alpha {}^C D_t^\alpha v(t) \quad (13)$$

which takes into account the non-local time behavior of the device, i.e. memory effects with respect to past activity up to a current generic time  $t$ .

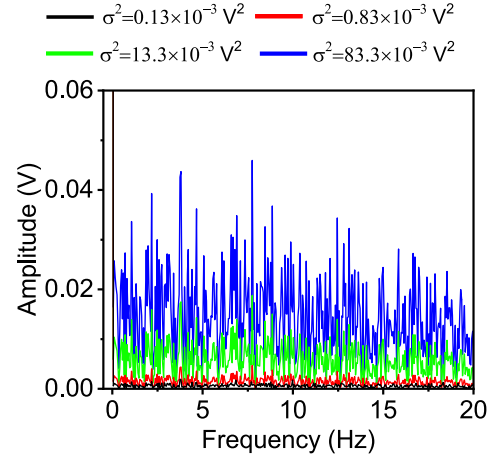


FIG. 3. Discrete-time Fourier transform (DTFT) of the voltage excitations in Fig. 2(a)

In a discretized form, the time-fractional derivative  ${}^C D_t^\alpha v(t)$  can be written in terms of finite difference approximation as follows [25]. For  $t_k = k\Delta t$ ,  $k = 0, 1, \dots, K$  and  $\Delta t = T/K$  is the time step, for all  $0 \leq k \leq K-1$  we have:

$${}^C D_t^\alpha v(t_{k+1}) \approx \frac{1}{\Gamma(2-\alpha)} \sum_{j=0}^k b_j \frac{v(t_{j+1}) - v(t_j)}{(\Delta t)^\alpha} \quad (14)$$

where  $b_j = [(k+1-j)^{1-\alpha} - (k-j)^{1-\alpha}]$ , with globally a  $(2-\alpha)$ -order accuracy in time [25]. Hence, Eq. 13 can be written as [14]:

$$\Delta q \approx \frac{C_0(\tau_0/\Delta t)^\alpha}{\Gamma(2-\alpha)} \{v(t_{k+1}) - v(t_k) + \sum_{j=0}^{k-1} b_j [v(t_{j+1}) - v(t_j)]\} \quad (15)$$

which is the the sum of the immediate past of the charge (first two terms, weighted by the Gamma function and the fractional time  $(\Delta t)^\alpha$ ) and a memory trace of the charge (last summation term) that contains voltage information about all previous activity of the device. The extent of the memory effect increases when the fractional order parameter  $\alpha$  in Eq. 15 decreases further away from one [13]. It is understood that at the limiting case of  $\alpha = 1$  corresponding to first order integer derivatives, the behavior of the differentiable function is determined just locally in an infinitesimal neighborhood of the considered point. In this case, the memory trace part is zero and does not have any effect on the dynamics of the device [13]. Thus, the relation  $\Delta q(t) = C_1 \Delta v$  can be said to do not carry memory information about past events endured by the device. However, lower values of  $\alpha$  explain the increased correlation between voltage and charge when higher magnitude of voltage fluctuations are subjected to the CPE-like device (Fig. 2). In fact, as the

magnitude of frequency components of the voltage input are increased with the increase of variance of the uniform noise (see DTFT of voltage excitations in Fig 3), the capacitive storage capability of the device is reduced as it becomes more and more resistive [26]. This can be deducted for instance from the increase of impedance phase with the increase of frequency as depicted in Fig. 1(b). Thus, because the value of  $\alpha$  decays with increasing frequency, the consequence is that the higher are the magnitudes of frequency components of the change in voltage (Fig. 3) the stronger is the effect of the memory trace term in Eq. 15.

## V. CONCLUSION

We have provided further experimental evidence of the inherent memory effect of EDLCs which results from the complex multi-time scale dynamics of their internal mi-

croscopic structure and mechanisms. The results shown here, in conjunction with the results reported in [11], indicate that it is possible to encode information in the statistical distribution of the random noise signal superimposed on the dc step charging voltage. From fractional modeling point of view, the memory effect or non-static, history-dependent input-to-output in such types of dissipative devices is attributed to stronger higher frequency harmonics of the input signal, and as a consequence to the extent of deviation of the device from ideality. In other words, high variance fluctuations makes the device operate in a less capacitive, more resistive mode with lower values of the fractional coefficient  $\alpha$ , and thus with a stronger memory trace that integrates all past values of its state.

## REFERENCES

- 
- [1] R. Metzler and J. Klafter, *Phys. Rep.* **339**, 1 (2000).
  - [2] H. Ribeiro and F. Potiguar, *Physica A* **462**, 1294 (2016).
  - [3] A. Allagui and H. Benaoum, *J. Electrochem. Soc.* **169**, 040509 (2022).
  - [4] A. Allagui, H. Benaoum, and O. Olendski, *Physica A*, 126252 (2021).
  - [5] A. Allagui, H. Benaoum, and C. Wang, *J. Phys. Chem. C* **126**, 3029 (2022).
  - [6] A. Allagui, H. Alnaqbi, A. S. Elwakil, Z. Said, A. Hachicha, C. Wang, and M. A. Abdelkareem, *Appl. Phys. Lett.* **116**, 013902 (2020).
  - [7] V. Uchaikin, R. Sibatov, and D. Uchaikin, *Physica Scripta* **2009**, 014002 (2009).
  - [8] V. Uchaikin, A. Ambrozevich, R. Sibatov, S. Ambrozevich, and E. Morozova, *Technical Physics* **61**, 250 (2016).
  - [9] A. Allagui, D. Zhang, and A. S. Elwakil, *Appl. Phys. Lett.* **113**, 253901 (2018).
  - [10] A. Allagui, D. Zhang, I. Khakpour, A. S. Elwakil, and C. Wang, *J. Phys. D* **53** (2020).
  - [11] A. Allagui and A. S. Elwakil, *Sci. Rep.* **11**, 1 (2021).
  - [12] M. Du, Z. Wang, and H. Hu, *Sci. Rep.* **3**, 3431 (2013).
  - [13] W. W. Teka, R. K. Upadhyay, and A. Mondal, *Neural Netw.* **93**, 110 (2017).
  - [14] W. Teka, T. M. Marinov, and F. Santamaria, *PLOS Comput. Biol.* **10**, e1003526 (2014).
  - [15] M. E. Fouda, A. Allagui, A. S. Elwakil, A. Eltawil, and F. Kurdahi, *J. Power Sources* **435**, 226829 (2019).
  - [16] A. Allagui, A. S. Elwakil, B. J. Maundy, and T. J. Freeborn, *ChemElectroChem* **3**, 1429 (2016).
  - [17] A. Allagui and M. E. Fouda, *Electrochim. Acta*, 138848 (2021).
  - [18] A. Allagui, T. J. Freeborn, A. S. Elwakil, M. E. Fouda, B. J. Maundy, A. G. Radwanh, Z. Said, and M. A. Abdelkareem, *J. Power Sources* **400** (2018).
  - [19] A. Allagui and H. Benaoum, *J. Electrochem. Soc.* (2022).
  - [20] R. Nigmatullin, *physica status solidi (b)* **124**, 389 (1984).
  - [21] A. Allagui, A. S. Elwakil, and C. Wang, *IEEE Trans. Circuits Syst. II Express Briefs* (2022).
  - [22] A. Allagui, A. S. Elwakil, and H. Eleuch, *J. Phys. Chem. C* **125**, 9591 (2021).
  - [23] A. Allagui, A. S. Elwakil, and M. E. Fouda, *IEEE Trans. Electron Devices* **68** (2021).
  - [24] D. Baleanu, A. K. Golmankhaneh, A. K. Golmankhaneh, and R. R. Nigmatullin, *Nonlinear Dynamics* **60**, 81 (2010).
  - [25] Y. Lin and C. Xu, *J. Comput. Phys.* **225**, 1533 (2007).
  - [26] A. Allagui, A. S. Elwakil, M. Fouda, and A. G. Radwan, *J. Power Sources* **390**, 142 (2018).